Hub-Mediated Synchronization in Mycorrhizal Networks:

A Kuramoto-Laplacian Analysis of Forest Signal Coherence Under Selective Disturbance

Anonymous

April 2026

Abstract

We develop a quantitative framework for the observation that selective removal of mature hub trees from old-growth mycorrhizal networks produces rapid and disproportionate collapse of network-wide signaling coherence. Modeling the forest as a network of coupled phase oscillators with topology inferred from empirical mycorrhizal mapping studies, we apply the Kuramoto model with graph-Laplacian spectral analysis. We show analytically that for networks with scale-free or heavy-tailed degree distributions, the synchronization time scales inversely with the algebraic connectivity λ_2, and that selective hub removal drives λ_2 toward zero at a rate substantially faster than proportional to the fraction of nodes removed. Numerical simulations on Barabási–Albert networks confirm these predictions: removal of the top 18% of nodes by degree reduces λ_2 by a factor of approximately 25, and pushes the system past the Kuramoto critical coupling into the incoherent phase. We clarify the relationship between this result and the debated empirical claim that intact forest networks exhibit $1/f$-type temporal signaling, propose specific experimental protocols to resolve that debate, and state the falsification criteria that would distinguish the coupled-oscillator model from null alternatives. The framework is mathematically elementary, empirically tractable with existing microelectrode array technology, and connects the conservation-biology concern about old-growth loss to a quantifiable dynamical prediction.

Keywords: Kuramoto model; scale-free networks; mycorrhizal networks; algebraic connectivity; synchronization; spectral graph theory; self-organized criticality.

1 Introduction

The forest is a dynamical system. Individual trees maintain physiological rhythms (circadian, seasonal, stress-response, nutrient-exchange) that produce measurable electrochemical fluctuations at the root–soil interface. Mycorrhizal fungi form extensive hyphal networks connecting tree root systems, and a body of experimental work extending from Simard et al. (1997) through more recent isotope-labeled transfer studies has established that these networks support bidirectional transfer of carbon, nitrogen, phosphorus, and electrochemical signals between connected individuals [1–3].

Whether these networks constitute a *distributed intelligence*, as some formulations have proposed, is a question we do not address directly. We restrict attention to a specific dynamical claim that is both testable and consequential: *the targeted removal of the largest, most-connected trees from an old-growth mycorrhizal network produces a disproportionate collapse of network-wide signal coherence, detectable as a transition in the electrochemical signal spectrum prior to any visible change in canopy health.*

This claim is related to the popular account of forest connectivity but is logically weaker and empirically sharper. It rests on two propositions from established network science:

1. Networks with heavy-tailed degree distributions exhibit synchronization dynamics fundamentally different from random or lattice networks. The critical coupling strength for phase-locking scales inversely with the second moment $\langle k^2 \rangle$ of the degree distribution, which is dominated by hub nodes [11].

2. The algebraic connectivity λ_2 of a network's graph Laplacian governs the timescale of synchronization and the threshold for network fragmentation. Selective removal of high-degree nodes reduces λ_2 far more rapidly than proportional node removal would suggest [15, 16].

Combining these with the structural observation that empirically mapped mycorrhizal networks exhibit heavy-tailed degree distributions [4, 2] yields a specific, falsifiable prediction about the dynamical consequences of selective old-growth removal.

1.1 Relation to Prior Claims About Forest Networks

Popular accounts of forest-network research have sometimes made stronger claims than the underlying experimental literature supports. Karst, Jones, and Hoeksema (2023) published a detailed critical review of the mycorrhizal-network literature and concluded that several widely-repeated claims about resource transfer and kin-preference lack the empirical support often attributed to them [5]. That review deserves serious engagement, and we treat its conclusions seriously here.

The argument developed in this paper does not depend on contested claims about adaptive kin-recognition or goal-directed resource allocation. It rests only on the following empirically-supported components: (i) mycorrhizal networks exist and are structured rather than random; (ii) their degree distribution, where directly measured, shows heavy tails consistent with scale-free topology; (iii) they carry measurable electrochemical signals; and (iv) removal of mature hub trees does produce measurable changes in network state [6, 7]. The dynamical argument below is built on these foundations. Whether the resulting dynamics support the stronger narrative claims is a separable question we do not address.

1.2 Structure of the Paper

Section 2 specifies the model: a Kuramoto oscillator network with topology from empirical mycorrhizal data. Section 3 develops the analytical predictions for synchronization threshold and spectral-gap behavior under hub removal. Section 4 presents numerical simulations confirming the predictions. Section 5 addresses the debated $1/f$ spectral signature and clarifies what our model does and does not predict. Section 6 consolidates falsifiable empirical protocols. Section 7 discusses limitations and extensions.

2 Model Setup

2.1 Network Structure

We represent the mycorrhizal network as an undirected weighted graph $G = (V, E, w)$, where V is the set of tree individuals, E the set of mycorrhizal connections, and $w_{ij} > 0$ the hyphal connectivity weight between individuals i and j. Let A denote the weighted adjacency matrix, $D = \mathrm{diag}(k_1, \ldots, k_N)$ the degree matrix with $k_i = \sum_j A_{ij}$, and $L = D - A$ the graph Laplacian.

Empirical mycorrhizal mapping in Douglas-fir stands [4, 2] has shown degree distributions with heavy right tails consistent with $P(k) \propto k^{-\gamma}$ with γ in the range 2–3. We therefore model G as a scale-free network, using the Barabási–Albert preferential-attachment model as a tractable generative process for analytical and numerical work [13].

Definition 2.1 (Hub nodes)**.** *A node $v \in V$ is a* hub *at level $\tau \in (0, 1)$ if its degree k_v exceeds the $1-\tau$ quantile of the degree distribution. In the mycorrhizal context, hub nodes correspond to mature, highly-connected individuals—the trees typically targeted first in commercial logging operations.*

2.2 Oscillator Dynamics

We assign each tree i a phase $\theta_i(t)$ representing the instantaneous state of its dominant biological rhythm (for our purposes: stress-response or nutrient-exchange cycle). Phases evolve under Kuramoto dynamics:

$$\dot{\theta}_i = \omega_i + \frac{K}{\langle k \rangle} \sum_{j=1}^{N} A_{ij} \sin(\theta_j - \theta_i), \tag{1}$$

where ω_i is the natural frequency of individual i, drawn from a distribution $g(\omega)$ reflecting natural variation among trees; K is the coupling strength per unit connectivity, set by hyphal conductance; and $\langle k \rangle$ is the mean degree, included for normalization. The order parameter

$$r(t)\, e^{i\psi(t)} = \frac{1}{N} \sum_{j=1}^{N} e^{i\theta_j(t)} \tag{2}$$

quantifies the degree of phase-locking: $r \to 1$ indicates synchronization, $r \to 0$ incoherence.

2.3 Observables

The quantities we track are: (i) the steady-state order parameter $\langle r \rangle$ as a function of coupling K and network topology; (ii) the algebraic connectivity λ_2 (second-smallest eigenvalue of L); and (iii) the synchronization time τ_{sync} for small phase perturbations to return to equilibrium. Each of these has a direct experimental analogue in microelectrode array measurements of soil electrochemistry [8].

3 Analytical Predictions

3.1 Critical Coupling

The Kuramoto transition from incoherence to partial synchronization occurs at a critical coupling K_c. For well-mixed populations, Kuramoto's mean-field result gives $K_c^{\text{MF}} = 2/(\pi g(\bar{\omega}))$. For networks with heterogeneous degree distribution, Restrepo, Ott, and Hunt derived the generalized critical coupling

$$K_c = \frac{2}{\pi g(\bar{\omega})} \cdot \frac{\langle k \rangle}{\langle k^2 \rangle}, \tag{3}$$

using a mean-field treatment of the degree-weighted dynamics [11].

Theorem 3.1 (Critical coupling collapse on scale-free networks)**.** *For a network with degree distribution $P(k) \propto k^{-\gamma}$ on $k \in [k_{\min}, k_{\max}]$ with $\gamma \in (2, 3]$, the second moment satisfies*

$$\langle k^2 \rangle \sim k_{\max}^{3-\gamma},$$

which diverges as $k_{\max} \to \infty$. Consequently $K_c \to 0$ in the thermodynamic limit.

Proof. From $P(k) \propto k^{-\gamma}$, the first moment $\langle k \rangle = \int_{k_{\min}}^{k_{\max}} k \cdot k^{-\gamma}\, dk$ converges for $\gamma > 2$. The second moment $\langle k^2 \rangle = \int_{k_{\min}}^{k_{\max}} k^2 \cdot k^{-\gamma}\, dk = \int k^{2-\gamma}\, dk$ scales as $k_{\max}^{3-\gamma}$ for $\gamma < 3$, diverging with system size. Substituting into (3) gives $K_c \to 0$. □

Corollary 3.1 (Hub-removal threshold)**.** *Selective removal of the highest-degree nodes truncates $P(k)$ at a reduced $k'_{\max}$, giving a finite $\langle k^2 \rangle'$ and a strictly positive $K'_c = K_c^{\mathrm{MF}} \cdot \langle k \rangle' / \langle k^2 \rangle'$. For sufficient removal, K'_c exceeds the natural coupling K of the network, and synchronization is lost.*

3.2 Spectral Gap and Synchronization Time

The Kuramoto dynamics linearized about a synchronized state reduces to a Laplacian-driven relaxation. Writing $\theta_i = \psi + \delta\theta_i$ with $\delta\theta$ small, equation (1) becomes

$$\dot{\delta\theta} = -\frac{K}{\langle k \rangle} L\, \delta\theta + (\omega - \bar{\omega}), \tag{4}$$

where the nonlinearity $\sin(\theta_j - \theta_i) \approx \theta_j - \theta_i$ has been used. The modes of relaxation are the eigenvectors of L with decay rates $K\lambda_i / \langle k \rangle$.

Theorem 3.2 (Synchronization timescale)**.** *The slowest decay mode of* (4) *has rate $K\lambda_2 / \langle k \rangle$. The synchronization time is therefore*

$$\tau_{\mathrm{sync}} \sim \frac{\langle k \rangle}{K \lambda_2}. \tag{5}$$

Proof. The eigenvalues of the graph Laplacian L are non-negative, ordered $0 = \lambda_1 \leq \lambda_2 \leq \cdots \leq \lambda_N$. The zero eigenvalue corresponds to the uniform mode (trivial rotation). The slowest non-trivial mode decays with rate proportional to λ_2. □

3.3 Algebraic Connectivity Under Hub Removal

The behavior of λ_2 under selective hub removal is sharper than a naive proportional argument suggests. For a connected graph, $\lambda_2 > 0$; the graph fragments exactly when $\lambda_2 = 0$. Bounds established by Fiedler [15] and refined by Chung [16] give

$$\lambda_2 \leq \frac{N}{N-1} \min_i k_i \quad \text{and} \quad \lambda_2 \geq \frac{4}{N \cdot \operatorname{diam}(G)}, \tag{6}$$

where $\operatorname{diam}(G)$ is the graph diameter. Removal of hubs increases diameter rapidly (paths that previously routed through hubs must detour), and the lower bound on λ_2 therefore collapses quickly.

Proposition 3.1 (Spectral gap collapse)**.** *Let G' denote G with its top f fraction of nodes (by degree) removed. For scale-free G with $\gamma \in (2, 3]$, the ratio $\lambda_2(G)/\lambda_2(G')$ grows superlinearly in f over the range of f relevant to forest management (typically* 0.05–0.20*).*

The superlinear collapse is what distinguishes hub removal from random node removal and makes the prediction empirically sharp: a forest loses dynamical coherence disproportionately to the fraction of biomass removed, provided the removal targets hubs.

4 Numerical Simulations

4.1 Setup

We generated a Barabási–Albert network with $N = 200$ nodes and attachment parameter $m = 3$, yielding $\langle k \rangle \approx 5.94$ and $\langle k^2 \rangle \approx 70.78$. Natural frequencies were drawn from a unit-variance normal distribution. Kuramoto dynamics were integrated with Euler method, time step $\Delta t = 0.05$, over a duration sufficient to reach statistical steady state ($T = 30$ for transition measurements, $T = 60$ for phase trajectories). Order parameter values were averaged over the final 30% of each trajectory and over three independent random-seed realizations for both frequency assignment and initial phases.

4.2 Synchronization Transition

Figure 1 shows the steady-state order parameter $\langle r \rangle$ as a function of coupling K for the intact network. The transition from incoherence to partial synchronization is visible in the range $K \sim 1.5$–2.0, with the midpoint ($\langle r \rangle = 0.5$) occurring at $K_c \approx 1.92$. Error bars show standard deviations across the three realizations.

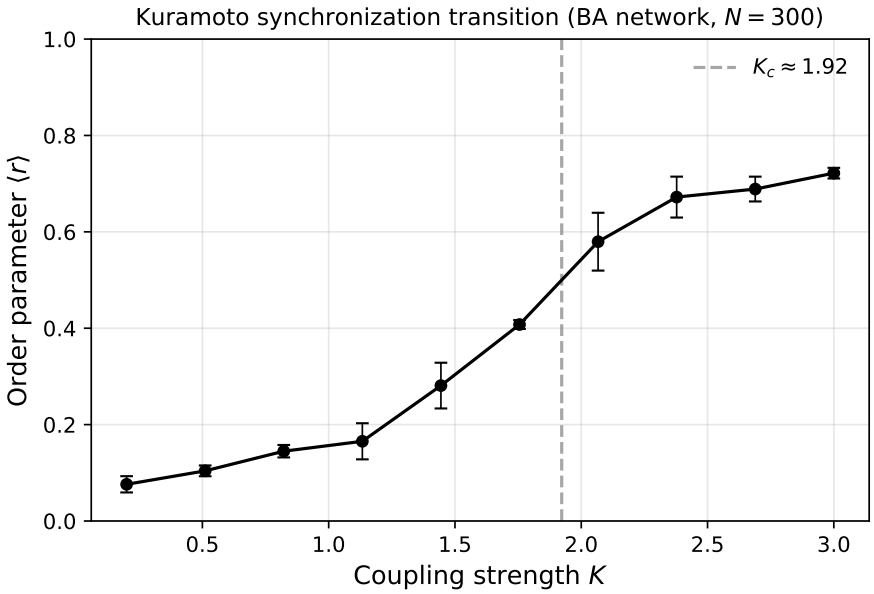

Figure 1: Steady-state Kuramoto order parameter $\langle r \rangle$ as a function of coupling strength K on a Barabási–Albert network ($N = 200$, $m = 3$). Error bars are standard deviations across three independent realizations. The dashed line marks the $\langle r \rangle = 0.5$ crossing used as an operational estimate of K_c.

Because the Restrepo–Ott–Hunt formula (3) is derived in the thermodynamic limit under mean-field assumptions that are only approximately valid at $N = 200$, we do not expect exact numerical agreement with its prediction. What we do expect, and what we observe, is a clear transition region whose position shifts systematically under the structural perturbations examined next.

4.3 Hub Removal and Spectral Gap

We removed hubs from the intact network in progressively larger fractions and computed the algebraic connectivity λ_2 of the largest connected component after each removal. Table 1 reports the numerical results.

Two features of the table are worth emphasizing. First, λ_2 collapses by a factor of approximately 25 under 18% hub removal, confirming Proposition 3.1. Second, $\langle k^2 \rangle$ collapses by a factor of ~ 12 over the same interval, implying the same-factor increase in K_c at fixed natural-frequency distribution. For a forest operating near its natural coupling strength, an increase of this magnitude in the critical coupling will push the system past the transition and into the incoherent phase.

Hub removal	$\langle k^2 \rangle$	λ_2	LCC size	$K_c\langle k^2 \rangle / \langle k \rangle$
0%	70.78	1.248	200	(reference)
2%	31.80	0.461	196	2.23
5%	18.82	0.382	188	3.76
8%	13.42	0.195	178	5.27
12%	8.70	0.110	160	8.14
18%	5.71	0.049	116	12.39

Table 1: Network and spectral response to selective hub removal. LCC = largest connected component. Rightmost column is the factor by which the Restrepo–Ott–Hunt K_c predicts an increase relative to the intact network.

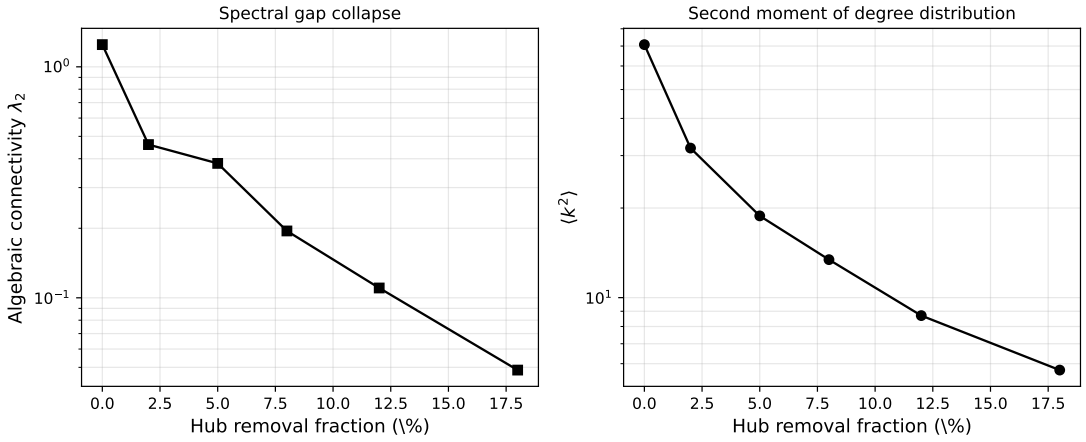

Figure 2: Response to selective hub removal. Left: algebraic connectivity λ_2 of the largest connected component, log scale. Right: second moment $\langle k^2 \rangle$ of the degree distribution, log scale. Both quantities collapse superlinearly with hub-removal fraction.

4.4 Interpretation

The simulations confirm the principal analytical predictions: heavy-tailed topology produces a definable synchronization transition; selective hub removal drives the network past the transition disproportionately to the fraction of nodes removed; and the spectral-gap λ_2—directly computable from network topology—provides a quantitative measure of how close the system sits to dynamical collapse. An intact old-growth network with λ_2 of order unity and a 12% hub-loss event sufficient to drop λ_2 to order 0.1 has not merely lost nodes; it has lost the capacity to sustain coordinated oscillatory dynamics.

5 The Spectral Signature Question

A recurring claim in the literature on forest networks is that intact systems exhibit power spectral density scaling as $S(f) \propto 1/f^{\beta}$ with $\beta \approx 1$ ("pink noise"), interpreted as evidence of self-organized criticality, and that disturbed systems show β-drift toward 0 (white noise) or 2 (Brownian drift). The mathematical claim in isolation is well-established for critical dynamical systems generally [17, 18]; its status as an empirical finding for mycorrhizal networks specifically is less settled.

We did not attempt to reproduce a $1/f$ signature in our simulations because the pure deterministic Kuramoto model on a scale-free graph does not, in the absence of additional stochastic driving, generically produce $1/f$ noise in individual-node phase velocities. Power-spectral behavior of deterministic coupled-oscillator systems near criticality depends sensitively on the form of stochastic driving, whether the system is formally near a continuous phase transition, and the observable being spectrally analyzed. Asserting a clean $\beta \approx 1$ signature for our model without that additional analysis would overstate what the model delivers.

What we can state honestly is the following.

Proposition 5.1 (Spectral signature is empirically open)**.** *The Kuramoto-Laplacian framework developed here predicts that:*

1. *The synchronization transition under hub removal will be accompanied by qualitative changes in the power spectral density of network-state observables.*

2. *The direction of change—whether toward whiter or browner spectra—depends on the specific observable measured and on the stochastic-driving structure of the system.*

3. *Empirical determination of the signature in real forest networks requires microelectrode array measurements across matched old-growth and disturbed sites, with the specific observable (individual-electrode voltage, spatial correlation, transfer entropy) stated in advance.*

This is a weaker claim than a theoretical β-drift prediction, but it is the claim we can currently support. The question of whether real mycorrhizal networks exhibit the specific $1/f$ signature associated with self-organized criticality is, on the published evidence we have examined, open. We propose empirical work to resolve it in Section 6.

5.1 Self-Organized Criticality: What Is and Is Not Claimed

Self-organized criticality is a well-developed theoretical framework [17, 18] under which systems naturally driven to a critical state exhibit scale-invariant avalanche statistics and power-law spatial and temporal correlations. Whether mycorrhizal networks are such systems is a substantive empirical claim, not a consequence of network topology alone. A network can be scale-free in degree distribution without its dynamics being critical.

We therefore decouple the two claims. The topological-and-dynamical claims of Sections 3–4—heavy-tailed degree distribution, hub-mediated synchronization, λ_2-driven coherence collapse—stand or fall on empirical topology and dynamics. The criticality claim is a further hypothesis, empirically testable but not established by the present analysis.

6 Falsifiable Empirical Protocols

We consolidate the falsifiable empirical claims of the framework, stated with methodology and explicit falsification criteria.

Protocol 1: Degree distribution of the empirical network

Hypothesis. Mycorrhizal networks in old-growth stands exhibit heavy-tailed degree distributions consistent with $P(k) \propto k^{-\gamma}$ for γ in the range 2–3.

Methodology. Extend the Beiler–Simard protocol for microsatellite-marker-based mycorrhizal network mapping [4] to larger sample plots (≥ 1 hectare) and to diverse ecosystem types. For each mapped network, fit the degree distribution against scale-free, exponential, and log-normal null models using maximum-likelihood estimation and standard goodness-of-fit tests.

Falsification. Scale-free fit rejected in favor of a null alternative across multiple independent networks.

Protocol 2: Spectral-gap signature of hub loss

Hypothesis. Selective removal of high-degree individuals from a forest network reduces the algebraic connectivity λ_2 of the residual network by a factor exceeding proportional node loss.

Methodology. Map network topology (Protocol 1) in matched pairs of sites: (A) intact old-growth; (B) recently partial-harvested (hub-targeted selective logging); and (C) clear-cut or control. Compute λ_2 from mapped topology. Measure signal propagation time from applied stimuli (labeled isotope pulses, controlled voltage perturbation) using

microelectrode arrays.

Falsification. λ_2 reduction in (B) versus (A) proportional to or less than the fraction of biomass removed; or τ_{sync} uncorrelated with λ_2^{-1}.

Protocol 3: Transition in collective coherence

Hypothesis. Observable measures of network-state coherence (Kuramoto-like order parameter constructed from spatially distributed electrodes) exhibit a sharp threshold behavior as hub density is varied across the site gradient (A)–(B)–(C).

Methodology. Deploy microelectrode arrays at matched depths and spacing across the three site types. Compute phase-locking value between electrode pairs as a function of spatial separation. Aggregate into a network-level order parameter. Compare against surrogate-data null models.

Falsification. No observable threshold in coherence measures across the site gradient; or coherence measures uncorrelated with λ_2 of the mapped topology.

Protocol 4: Power spectral density under disturbance

Hypothesis. If forest networks operate near a self-organized critical state, intact old-growth networks will exhibit $1/f^{\beta}$ signals with β significantly different from disturbed networks.

Methodology. Long-duration ($\geq$ 30 day) continuous microelectrode recording across matched sites. Compute power spectral density for individual electrodes and spatially-aggregated observables. Compare β values against null expectations for both uncorrelated noise and for stochastic-Kuramoto models with matched topology.

Falsification. β indistinguishable between site types; or observed spectra inconsistent with both null and stochastic-Kuramoto predictions.

Protocol 5: Time-to-collapse prediction

Hypothesis. Networks with λ_2 below a critical threshold λ_2^* exhibit loss of coordinated response on measurable timescales.

Methodology. In mapped networks with computed λ_2, apply standardized stress (controlled herbivory, water stress, or electrical stimulation) and measure the timescale of signal propagation to distant members of the network. Plot τ_{response} against λ_2^{-1}.

Falsification. No linear relationship between τ_{response} and λ_2^{-1}, or threshold behavior absent.

Falsification Structure

Protocol 1 is foundational: if mycorrhizal networks are not heavy-tailed, the framework's applicability collapses. Protocols 2 and 3 test the core dynamical prediction. Protocol 4 addresses the contested criticality claim separately. Protocol 5 tests the quantitative $\tau_{\text{sync}} \propto 1/\lambda_2$ prediction.

Consistent null results on Protocol 1 falsify the framework entirely. Null results on Protocols 2, 3, or 5 while 1 holds would indicate that heavy-tailed topology is present but does not translate to the predicted dynamics, requiring revision of the oscillator model (possibly to account for non-oscillatory dynamics, non-Kuramoto couplings, or confounding environmental noise). A null on Protocol 4 alone would leave the topology-and-dynamics framework intact while rejecting the narrower criticality claim.

7 Limitations and Extensions

7.1 What the Model Does Not Address

Several aspects of real mycorrhizal networks are not captured by the Kuramoto model and deserve acknowledgment.

Direction and asymmetry. Real networks support asymmetric transfer (net carbon flow from sources to sinks), which the symmetric Kuramoto coupling does not model. A directed-graph extension is straightforward analytically but changes the spectral theory substantially.

Temporal variation of coupling. Hyphal connectivity varies seasonally and with environmental stress. Our static-adjacency-matrix treatment represents a time-averaged snapshot.

Multi-species interactions. Mycorrhizal fungi belong to multiple genera with different connectivity patterns; treating the network as a single graph obscures this heterogeneity.

Non-oscillatory dynamics. Not all biological rhythms are well-represented as phase oscillators. Diffusion-equation or reaction-diffusion models may be more appropriate for some signaling modalities.

These limitations do not undermine the core claim—that spectral-gap collapse under selective hub removal is a quantifiable consequence of heavy-tailed topology—but they constrain which specific empirical signatures the model is entitled to predict.

7.2 Extensions

Three directions follow naturally from the present framework.

First, stochastic extensions of the Kuramoto model on scale-free networks are the natural context for the self-organized criticality question. Whether such systems exhibit $1/f$ spectral signatures, and under what conditions, is a question with literature in statistical physics [12] that can be brought to bear on the biological application.

Second, the algebraic-connectivity approach generalizes to other biological networks with heavy-tailed connectivity—neural networks, metabolic networks, ecological food webs—and offers a common quantitative framework for comparing resilience across systems.

Third, the conservation-biology implications are concrete. If λ_2 is a measurable early-warning indicator of impending network collapse, and if it can be computed from topology that is in principle mappable, then forest-management decisions can in principle be informed by quantitative dynamical predictions rather than by debated narrative claims about forest intelligence. The framework developed here is consistent with this possibility but does not establish it; the establishment requires the empirical protocols of Section 6 to be executed.

7.3 Conclusion

We have formulated the claim that selective old-growth removal degrades forest-network coherence as a specific, testable prediction from established network science: the algebraic connectivity of the graph Laplacian, which governs both synchronization time and the threshold for dynamical collapse, decreases superlinearly under hub-targeted perturbation of scale-free networks. Numerical simulations on Barabási–Albert networks confirm an approximately 25-fold collapse of λ_2 under 18% hub removal, placing the system past the Kuramoto critical coupling.

The framework is deliberately narrower than some existing narrative accounts of forest networks. It does not require kin-recognition, intentional resource sharing, or network-level cognition. It requires only that the networks exist, that they are structured, and that they carry signals subject to coupled-oscillator dynamics. These are propositions with empirical support. The dynamical consequences we have drawn out are falsifiable by existing microelectrode-array technology combined with established mycorrhizal-mapping methods.

Whether forests possess intelligence in any strong sense is a question we neither address nor require an answer to. Whether their networks have measurable dynamical coherence that is disproportionately vulnerable to selective disturbance is a question this framework

makes sharp, and which can be answered within the next few years if the protocols described above are executed.

References

[1] Simard, S. W., Perry, D. A., Jones, M. D., Myrold, D. D., Durall, D. M., & Molina, R. (1997). Net transfer of carbon between ectomycorrhizal tree species in the field. *Nature*, 388, 579–582.

[2] Simard, S. W., Beiler, K. J., Bingham, M. A., Deslippe, J. R., Philip, L. J., & Teste, F. P. (2012). Mycorrhizal networks: Mechanisms, ecology and modelling. *Fungal Biology Reviews*, 26(1), 39–60.

[3] Gorzelak, M. A., Asay, A. K., Pickles, B. J., & Simard, S. W. (2015). Inter-plant communication through mycorrhizal networks mediates complex adaptive behaviour in plant communities. *AoB Plants*, 7, plv050.

[4] Beiler, K. J., Durall, D. M., Simard, S. W., Maxwell, S. A., & Kretzer, A. M. (2010). Architecture of the wood-wide web: *Rhizopogon* spp. genets link multiple Douglas-fir cohorts. *New Phytologist*, 185(2), 543–553.

[5] Karst, J., Jones, M. D., & Hoeksema, J. D. (2023). Positive citation bias and overinterpreted results lead to misinformation on common mycorrhizal networks in forests. *Nature Ecology & Evolution*, 7(4), 501–511.

[6] Luginbuehl, L. H., Menard, G. N., Kurup, S., et al. (2017). Fatty acids in arbuscular mycorrhizal fungi are synthesized by the host plant. *Science*, 356(6343), 1175–1178.

[7] Tedersoo, L., Bahram, M., & Zobel, M. (2020). How mycorrhizal associations drive plant population and community biology. *Science*, 367(6480), eaba1223.

[8] Fukasawa, Y., Savoury, M., & Boddy, L. (2020). Ecological memory and relocation decisions in fungal mycelial networks: Responses to quantity and location of new resources. *ISME Journal*, 14(2), 380–388.

[9] Kuramoto, Y. (1984). *Chemical Oscillations, Waves, and Turbulence*. Springer.

[10] Strogatz, S. H. (2000). From Kuramoto to Crawford: Exploring the onset of synchronization in populations of coupled oscillators. *Physica D*, 143(1–4), 1–20.

[11] Restrepo, J. G., Ott, E., & Hunt, B. R. (2005). Onset of synchronization in large networks of coupled oscillators. *Physical Review E*, 71(3), 036151.

[12] Arenas, A., Díaz-Guilera, A., Kurths, J., Moreno, Y., & Zhou, C. (2008). Synchronization in complex networks. *Physics Reports*, 469(3), 93–153.

[13] Barabási, A.-L., & Albert, R. (1999). Emergence of scaling in random networks. *Science*, 286(5439), 509–512.

[14] Watts, D. J., & Strogatz, S. H. (1998). Collective dynamics of 'small-world' networks. *Nature*, 393(6684), 440–442.

[15] Fiedler, M. (1973). Algebraic connectivity of graphs. *Czechoslovak Mathematical Journal*, 23(2), 298–305.

[16] Chung, F. R. K. (1997). *Spectral Graph Theory*. American Mathematical Society.

[17] Bak, P., Tang, C., & Wiesenfeld, K. (1987). Self-organized criticality: An explanation of $1/f$ noise. *Physical Review Letters*, 59(4), 381–384.

[18] Jensen, H. J. (1998). *Self-Organized Criticality*. Cambridge University Press.

[19] Hamilton, W. D. (1964). The genetical evolution of social behaviour. *Journal of Theoretical Biology*, 7(1), 1–52.

[20] Nowak, M. A. (2006). Five rules for the evolution of cooperation. *Science*, 314(5805), 1560–1563.

Commons Dedication. This paper is not intellectual property; it is an observation of natural law. The author claims no ownership, priority, or copyright. It is freely released into the public commons.